Failure of bivalve foundation species recruitment related to trophic changes during an extreme heatwave event

Alana Correia-Martins, Réjean Tremblay, Béatrice Bec, Cécile Roques, Ariane Atteia, Angélique Gobet, Marion Richard, Masami Hamaguchi, Toshihiro Miyajima, Masakazu Hori, et al.

Failure of bivalve foundation species recruitment related to trophic changes during an extreme heat wave event

Alana Correia-Martins[1], Réjean Tremblay[1], Béatrice Bec[2], Cécile Roques[2], Ariane Atteia[3], Angélique Gobet[3], Marion Richard[3], Masami Hamaguchi[4], Toshihiro Miyajima[5], Masakazu Hori[4], Gilles Miron[6], Stéphane Pouvreau[7], Franck Lagarde[3*]

[1]Institut des sciences de la mer, Université du Québec à Rimouski, 310 allée des Ursulines, G5L 3A1, Rimouski, QC, Canada

[2]MARBEC, Univ Montpellier, CNRS, Ifremer, IRD, Montpellier, France

[3]MARBEC, Univ Montpellier, CNRS, Ifremer, IRD, Sète, France

[4]National Research Institute of Fisheries and Environment of Inland Sea, Fisheries Research Agency, Maruishi 2-17-5, Hatsukaichi, Hiroshima 739-0452, Japan

[5]Marine Biogeochemistry Group, Atmosphere and Ocean Research Institute, University of Tokyo, Kashiwanoha 5-1-5, Kashiwa, Chiba 277-8564, Japan

[6]Département de biologie, Université de Moncton, 18 avenue Antonine-Maillet, E1A 3E9 Moncton, NB, Canada

[7]UMR LEMAR 6539, IFREMER, Argenton-en-Landunvez, France

*Corresponding author

ABSTRACT

Bivalves are regulators of coastal lagoons and provide a wide range of ecosystem services. However, coastal lagoons are sensitive to climate change. Our objective was to describe the drivers of the cascade of ecological events that occurred during a summer heat wave and resulted in recruitment failure of the oyster *Crassostrea gigas*. Results showed elevated temperature and salinity caused a shift in planktonic food availability toward smaller taxa. These trophic changes did not affect food accumulation by oyster larvae or their fatty acid composition but did affect post-metamorphosis success, as their gill development was not adapted to these small particles. This resulted in the failure of oyster recruitment and stimulated the development of annelids, a trophic and spatial competitor that can better ingest small particles. This knowledge suggests that in the context of marine heat waves, the ecological limits of oyster larvae are narrower than their physiological limits.

KEYWORDS

Climate change, Phenology, Extreme Heat Wave, Bivalves, Pacific Oyster, *Crassostrea gigas*, Reproduction, Larval Ecology, Cascade of Environmental Effects, Trophic Changes.

1. INTRODUCTION

Coastal lagoons provide a wide range of ecosystem services (Chapman 2012, Villamagna et al. 2013, Kermagoret et al. 2019), associated with biodiversity, including bivalves which are of great ecological interest and high commercial value for some of them. Bivalves also have an important regulatory functions in the ecosystem thanks to their capacity to extract particles, to regenerate and store nutrients and to form hard biogenic structures (Smaal et al. 2019). However, because coastal lagoons are shallow and have limited exchange with the ocean, they are highly sensitive to eutrophication, heat waves, hypoxia and acidification, as well as to the effects of global climate change (Lloret et al. 2008, Lu et al. 2018, Thomas et al. 2018). An atmospheric heat wave is defined as five consecutive days with a maximum temperature 5°C above the 1976-2005 normal (Jouzel et al. 2014). Summer 2019 was characterized by two heat waves of exceptional intensity over France, including the Thau Basin, one from June 24 to July 7, the other from July 21 to 27. The absolute heat record for France (46 °C) was measured in Vérargues in the Hérault administrative department (Météo-France 2019), which includes the Thau basin. Marine heatwaves (MHW) are extreme events defined as abrupt but prolonged periods of high sea surface temperatures that can occur anywhere, at any time (Scannell et al. 2016, Schlegel et al. 2017, Hobday et al. 2018). High water temperatures increase the metabolic requirements of bivalves (Filgueira et al. 2016, Thomas & Bacher 2018). Even if temperatures remain within the species' thermal range, high temperatures combined with salinity and/or food variations, can negatively impact the life cycle of bivalves (Filgueira et al. 2016).

Several studies suggest that global changes are disrupting plankton communities and their nutritional values by affecting the abundance, size and diversity of primary producers

(Klauschies et al. 2012, Sommer et al. 2012, Trombetta et al. 2019). Generally, elevated temperatures affect phytoplankton cell size with a shift from larger to smaller species (Bec et al. 2005, Trombetta et al. 2019). Adult bivalves can assimilate small phytoplanktonic particles (Sonier et al. 2016). However, the efficiency of the capture is regulated by the morphology of their gills, and is generally low when small particles as picoplankton are present (Rosa et al. 2018). Larvae feed through a less selective velum (Bower & Meyer 1990). Marine phytoplankton species are major producers of long-chain polyunsaturated essential fatty acids (EFA) but are predicted to decrease due to ocean warming (Hixson & Arts 2016, Colombo et al. 2017). The fatty acids docosahexaenoic acid (22:6ω3; DHA), eicosapentaenoic acid (20:5ω3; EPA) and arachidonic acid (AA) are essential for the growth and survival of marine invertebrates, particularly during their metamorphosis from pelagic larvae to benthic juveniles and ultimately, their recruitment success (Gagné et al. 2010, Bassim et al. 2015). Since EFAs are poorly biosynthesized by marine animals, their intake depends on their food (Glencross 2009, Da Costa et al. 2015). Thus, both the right size and the right fatty acid composition of larval food are essential for the recruitment success of bivalves.

The aim of this study was to identify the environmental factors and trophic conditions (Supplementary material table1 & table 2) associated with the recruitment failure of the Pacific oyster, *Crassostrea gigas*, during a heat wave. We compared two contrasted years (2017 no heat wave and 2019 heat wave) in four sites in the Thau lagoon, France (Fig. 1). We hypothesize that the heat waves, characterized by high temperatures and high salinity, have a negative impact on oyster recruitment due to poor larval feeding conditions caused by changes in plankton diversity.

2. MATERIALS AND METHODS

2.1 Experimental design

Oyster recruitment was monitored from July 24 to August 21, 2017, and from July 2 to 29, 2019, at four experimental sites in the Thau lagoon (southern France; Fig 1.). The average depth of the lagoon is 4 m. The lagoon covers an area of 7 500 ha (19 km x 4.5 km) of which 20% is used for shellfish culture (oysters and mussels). The lagoon is connected to the Mediterranean Sea via a network of channels through Sète Harbor(Fiandrino et al. 2017). Two experimental sites were located inside the shellfish farming areas (Marseillan and Bouzigues) while two others were located outside the shellfish farming areas (Meze and Listel) (Fig 1.).

2.2 Oyster analyses

Three sets of oyster collectors were submerged vertically 2 m below the surface at each of the four study sites in the Thau lagoon to collect young settlers (pediveligers settled on collectors, metamorphosed juveniles, and newly metamorphosed juveniles). The collectors were installed once the oyster's larval supply reached a density of 10 000 larvae/m^3 (VELYGER network[44]). The collectors located inside the shellfish culture areas were suspended from existing farming structures. Those outside the area were suspended using a mooring system (Lagarde et al. 2017, 2019). Each collector was made of 44 white PVC plastic plates (15 cm diameter; surface area of 250 cm^2) stacked on a 110 cm tube. Two weeks after their immersion, three plates per collector were harvested [at the top (i.e., the 5^{th} from the surface), in the middle (the 22^{nd}) and at the bottom (the 39^{th})] and data were pooled to assess the abundance of young settlers and fatty acid (FA) content (µg $larva^{-1}$). A similar sampling procedure was used four weeks after the collectors were immersed to assess the abundance of juveniles.

The abundance of young settlers and juveniles was assessed on the upper surface of each plate using standard 15 cm^2 sub-units. Depending on the abundance, 3 to 12 sub-units were randomly selected for counting and the resulting replicates were averaged to obtain the total number of individuals per plate. Recruitment was evaluated from the abundance of juveniles and metamorphosis from the ratio of juvenile to young-settler abundances. Size at metamorphosis was estimated by measuring the prodissoconch II (PII) (Martel et al. 1995). A maximum of 60 spats were removed from each plate sampled after the fourth week after immersion, and placed on a plasticine flange fixed on a microscope blade. Observations were made under the wide-range zoom lens of a high-resolution digital microscope Keyence (VHX 2000E, 1 μm resolution, HDR images), and the maximum dorsoventral axis was measured. This measurement corresponds to the distance between the umbo and the most distant part of the clear demarcation formed by a growth line delimiting the PII from the dissoconch shell.

The fatty acid (FA) composition of young settlers was determined using a pool of 77 to 212 individuals per replicate (2-3 replicates per site depending on pediveliger abundances). Samples were preserved in vials with 3 mL of dichloromethane methanol (CH_2Cl_2:MeOH, 2:1 v:v), closed with a Teflon-lined cap under nitrogen atmosphere and stored at -80 °C until analysis. Lipids were extracted by grinding in dichloromethane methanol using a modified Folch procedure (Parrish 1999). Fatty acid methyl esters (FAME) were prepared using sulfuric acid and methanol (2:98 v:v) at 100 °C for 10 min and using 19:0 as internal standard (Lepage & Roy 1984). Samples were purified on an activated silica gel with 1 mL of hexane ethyl acetate (v:v) to eliminate free sterols. FAME were analyzed in the full scan mode (ionic range: 50–650 m:z) on a Polaris Q ion trap coupled to a Trace GC Ultra gas chromatograph (Thermo Scientific)

equipped with a TriPlus autosampler, a PTV injector and an ITQ900 mass detector (Thermo Scientific). An Omegawax 250 (Supelco) capillary column was used for separation using high purity helium. Xcalibur v.2.1 software (Thermo Scientific) was used for FAME identification and quantification with the standards (Supelco 37 Component FAME Mix and Supelco menhaden oil). Unknown peaks were identified according to their mass spectra with emphasis on FA trophic makers.

2.3 Environmental measurements

Environmental factors were measured once a week (supplementary files table 1 and table 2) just after immersion of the collectors until the plates were harvested, i.e., a total of five weeks. Temperature (°C), salinity (PSU) and dissolved oxygen concentrations (mg L^{-1}) were measured at a depth of 1 m and at the bottom of the water column with an Oxi1970i WTW oximeter and an LF 197-S WTW conductivity meter.

Potential food for oysters is expressed as the concentration of total suspended particulate matter varying in size from 0.7 and 20 µm ($TPM_{0.7\text{-}20\mu m}$, mg L^{-1}). It consisted of inorganic ($PIM_{0.7\text{-}20\mu m}$, mg L^{-1}) and organic particulate matter ($POM_{0.7\text{-}20\mu m}$, mg L^{-1}). Once a week, three replicate water samples were collected at a depth of 1 m using a Ruttner Standard Water Sampler (Hydro-Bios Apparatebau) and stored at 4 °C for less than 2 hours before filtration for the measurement of the concentrations (mg mL^{-1}) of pico and nano-seston. In 2017, 500-mL subsamples of 1-L samples were used for filtration, while 1-L subsamples of 2-L samples were used in 2019. Water samples were first filtered by gravity through a Nuclepore membrane (20 µm pore size). Fractioned water samples were then filtered using a vacuum pressure pump (0.3 bar) on pre-

weighed (Mettler Toledo XP6 microbalance) pre-combusted (at 500 °C) Whatman 25 mm GF/F filters (0.7 µm pore size). The GF/F filters were rinsed with an isotonic seawater solution of ammonium formate (38 g L^{-1} distilled water) to eliminate salt deposits and stored in Millipore™ PetriSlide™ containers at - 25°C. The filters were dried at 70 °C for 24 h, weighed and the concentration of total particulate matter $TPM_{0.7\text{-}20\mu m}$ was determined. The filters were then combusted at 500 °C for 5 h and reweighed to determine the concentration of particulate inorganic matter ($PIM_{0.7\text{-}20\mu m}$, mg L^{-1}). The concentration of particulate organic matter ($POM_{0.7\text{-}20\mu m}$, mg L^{-1}) was the difference in weight between the dried and the combusted filter. To determine the FA content of the pico- and nano-seston (µg.mg $TPM_{0.7\text{-}20\mu m}^{-1}$), 1-L water samples collected in 2017 and 2-L water samples collected in 2019 were filtered as described above without addition of ammonium formate solution. GF/F filters were stored in 3 ml of CH_2Cl_2:MeOH (2:1 v:v) under a nitrogen atmosphere in vials with a Teflon-lined cap and stored at -80 °C. The mass of total fatty acids in the seston (MTFA; µg mg^{-1} POM) and its composition (% fatty acids) were obtained as already described for oysters, with lipid extraction carried out by sonification rather than grinding.

Plankton diversity was collected in 1-L samples in 2017 and in 2-L samples in 2019 collected weekly with a Ruttner Standard Water Sampler (Hydro-Bios Apparatebau) at each sampling site. This sampling strategy provided 40 observations (4 sites x 5 weeks x 2 years). Phytoplankton was characterized using the standard Utermöhl method NF-EN-152014, 2006 in 10 mL seawater samples. Abundances are expressed as the number of individuals per liter in 52 diatom taxa and 38 dinoflagellate taxa. Chlorophyll *a* (Chl-*a*), *b* (Chl-*b*) and *c* (Chl-*c*) biomasses were evaluated in 200 ml seawater samples filtered (Bec et al. 2005, 2011) on Whatman GF/F

membranes (0.7 μm pore size) with a vacuum pressure pump (<10 cm Hg). Filters were stored in glass tubes at -20 °C until analysis. To determine the contribution of picophytoplankton (<3 μm), nanophytoplankton (3 to 20 μm) and microphytoplankton (>20 μm), two out of three samples were size-fractioned beforehand by gravity through Nuclepore membranes (3 and 20 μm pore size). Filters were ground in acetone (90%) and extracted at 4 °C for 24 h in the dark. Pigment contents were measured with a spectrofluorometer (Perkin-Elmer LS50b) (Neveux & Lantoine 1993) and are expressed in μg chl *a* L^{-1}. Concentrations of picocyanobacteria (<1 μm), autotrophic picoeukaryotes (<3 μm), nanophytoplankton (3-20 μm) and bacteria were estimated using a FACSCalibur flow cytometer Becton Dickinson methods (Marie et al. 1997, Bec et al. 2011). Seawater samples (1-ml) were analyzed; abundances are expressed in cells per liter. Total picophytoplankton abundances were assessed by summing picocyanobacteria and photosynthetic picoeukaryote abundances. Fluorescent beads (0.94 μm; 2 and 3 μm, Polysciences) were added to each sample. To measure bacterial abundances, seawater samples were fixed with prefiltered (0.2 μm) buffered formaldehyde (2% final concentration) and stored in liquid nitrogen. The procedure was slightly modified as higher concentrations of fluorochromes (SYBR Green I) were used (Bouvy et al. 2016). The fixed samples were incubated with SYBR Green I (Molecular Probes) at a final concentration of 1/375 at 4 °C for 15 min in the dark. Stained bacterial cells excited at 488 nm were determined according to their side-scattered light and green fluorescence collected using a 530/ 30 nm filter. Fluorescent beads (0.94 μm; Polysciences) were added to each sample.

Protozooplankton (heterotrophic flagellates) abundances were determined using the standard 2006 Utermöhl method NF-EN-152014, and are expressed in cells per liter. Until used for heterotrophic flagellate analysis, 30-ml seawater samples were preserved with 2.5-ml of

prefiltered (0.2 μm) formaldehyde and kept at 4 °C in the dark. Before counting, 10 ml subsamples were stained with 4',6-diamidino-2-phenylindole (DAPI) for a final concentration of 2.5 μg ml^{-1}. Heterotrophic flagellates were counted by size class (2-5 μm, 5-10 μm and >10 μm) under an epifluorescence microscope (Olympus AX70) with UV illumination (Sherr et al. 1993).

2.4 Territorial competition

Percent cover of tubeworm (*Ficopomatus enigmaticus*) on plates sampled in the fourth week after immersion (6 plates per site) was estimated to assess territorial competition with oyster juveniles, but only during the 2019 sampling season, as no tubeworms were observed in 2017. Photographs of each plate were taken with a GoPro HERO4 Silver camera equipped with a macro pro filter (San Mateo, CA, USA) and the % of tubeworms recovered on the plate was estimated using Image-Pro Insight 9.1 software (MediaCybernetics, Rockville, MD, USA).

2.5 Statistical analyses

All PERMANOVA analyses were performed with Primer 7 and Permanova+1 (version 7.0.13) software. A two-way PERMANOVA (n perm.: 9999) was conducted using a Euclidian distance matrix to test the effect of year (2 fixed levels) and sampling site (4 fixed levels) on size at metamorphosis, total and essential fatty acid contents in young settlers and on all the environmental variables measured, except the oxygen level, which was added as a third factor (depth) in the analysis. Homogeneity was evaluated using the permutation analysis of multivariate dispersion (PERMDISP) routine. When significant PERMANOVAs were observed, post hoc multiple comparison tests were carried out. Multivariate analyses of total

FA composition in young settlers and in seston, including *a posteriori* pairwise comparison, were done using distance-based permutational multivariate analysis of variance (PERMANOVA, 9999 permutations) based on Euclidian dissimilarities with year (2 fixed levels) and sampling site (4 fixed levels) as sources of variation. Variations in FA composition, expressed in percentages, were visualized using non-metric multidimensional scaling (n-MDS). The similarity percentages (SIMPER) procedure was performed on untransformed data to identify the FAs that explained the most dissimilarity between significant different levels.

3. RESULTS

3.1 Oyster recruitment

Recruitment numbers showed dramatic annual variability with great success at some sites in 2017 but an overall near-zero recruitment level at all sites in 2019 (Fig. 2a, b). In 2017, the metamorphosis survival rate, expressed as the ratio of juvenile to young settler abundances per plate, also showed marked spatial variability. The ratio of juvenile (123 ± 9 ind. plate^{-1}) to young-settler abundances per plate (49 ± 6 ind. plate^{-1}) was 2.5 in Bouzigues, suggesting up to 100% successful metamorphosis by competent larvae and the arrival of competent larvae from elsewhere. However, in the other sites, recruitment level decreased by 24% (94 ± 16 juveniles plate^{-1}) in Meze, 90% (13 ± 2 juveniles plate^{-1}) in Listel, and 97% (4 ± 2 juveniles plate^{-1}) in Marseillan. A poorer supply of larvae (6 ± 2 young-settlers plate^{-1}) was observed in Marseillan, but the metamorphosis survival rate was 0.6. However, in Meze and Listel, the low recruitment rates were not linked to the supply of larvae, as young settler abundances were higher in Meze (328 ± 71 young settler plate^{-1}, with a metamorphosis survival rate of 0.3) and in Listel (670 ± 65 young settler plate^{-1}, with a metamorphosis survival rate of 0.02) than in Bouzigues. Failure

characterized the 2019 oyster recruitment season: low abundances of young settlers were observed in Meze (116 ± 5 ind. plate^{-1}) and in Listel (31 ± 2 ind. plate^{-1}), with almost 3 and 22 times fewer individuals than in 2017, respectively. This trend was not observed in Bouzigues (84 ± 9 ind. plate^{-1}) or in Marseillan (45 ± 3 ind. plate^{-1}) in 2019. Instead, young settlers were respectively 2 and 7 times higher in 2019 than in 2017. However, two weeks later, almost no juveniles were observed on the plates (average 0.14 ± 0.06), regardless of the sites, pointing to a general oyster recruitment failure in 2019.

The size of juveniles at metamorphosis (PII length) was established in all samples, except samples from Bouzigues in 2019 (Fig 2c, d), in which no metamorphosis of young settlers to juveniles was observed. PII individuals sampled in 2019 were 5.1% smaller (mean 262 ± 1 µm) than those sampled in 2017 (mean 276 ± 1 µm). Differences among sites were only observed in 2017, when PII sizes in Bouzigues were 2.7% smaller than those in Meze ($p = 0.02$), Listel ($p = 0.01$) and Marseillan ($p = 0.03$).

No differences in total fatty acid (TFA) contents were observed in young settlers in the four sites and the two years. The overall TFA average was 51 ± 19 ng lavae^{-1} ($p > 0.06$). The sum of essential fatty acids (EFA) corresponded to about 10% of TFA with an effect of year × site (df=3 and 19, pseudo-F=6.47, p=0.007), as individuals in Listel (p=0.02) and Marseillan (p=0.006) had 5 times lower TFA contents in 2017 than in 2019. The fatty acid composition of young settlers varied with the year × site interaction (df=3 and 19, pseudo-F=2.34, p=0.017), as individuals sampled in Listel (p=0.047) and Marseillan (p=0.044) had different profiles in the two years (Supplementary material Fig. 1). According to SIMPER analysis, the interannual differences observed at these two sites were linked to DHA (22:6n3), EPA (20:5n3), AA (20:4n6), 18:2n6, 18:0 and 16:0 explained more than 83% of the average dissimilarity in the

fatty acid profiles. DHA, EPA and AA levels in young settlers sampled in 2019 were twice higher than in 2017, while the levels of 18:2n6 were five times lower in 2019 than in 2017, except for the Meze and Bouzigues sites ($p > 0.09$).

3.2 Physico-chemical parameters

Average water temperatures were 2.6°C higher and salinity was 0.34 S higher in 2019 than in 2017 (Fig 3a, b, Supplementary Table 3 and Supplementary Table 4). A site effect was also observed for salinity in the Thau lagoon. Salinity increased from east to west: the mean value at Marseillan was 0.68 S higher than at Bouzigues. Conversely, no effect of site on temperature was observed. There was a site × year effect on oxygen concentration (Supplementary Table 5). No difference was observed among sites in 2017 (c). The lowest values were observed in Bouzigues in 2019 ($p = 0.001$) near the bottom of the lagoon (21.8% lower than in 2017). Oxygen concentrations varied with water depth, lower values generally being observed near the bottom (Fig. 3c).

3.3 Potential food for oyster larvae

Concentrations of $TPM_{0.7\text{-}20}$ (), $PIM_{0.7\text{-}20}$ () and $POM_{0.7\text{-}20}$ () were more than twice higher in 2019 than in 2017 (Fig. a, b, c, Supplementary Table 6, 7 and 8). Significant differences among the four sites were only observed in $POM_{0.7\text{-}20}$ concentrations. In both years, $POM_{0.7\text{-}20}$ concentrations in Marseillan were 0.7 and 0.8 times lower than in Listel and Meze ($p = 0.01$ and 0.03 respectively). An effect of year × chl-*a* biomasses fraction was observed (Supplementary Table 9). Mean nanophytoplankton and picophytoplankton biomasses ($p = 0.0001$ and $p = 0.0004$ respectively) were 3 times higher in 2019 (Fig.4d, e) than in 2017. A site × year

effect was also observed, chl-*a* biomass values were 45% lower in Bouzigues than in Listel (p=0.01) and Meze (p = 0.004) in 2017. In 2019, biomasses in Marseillan were 62% lower than at the other sites (p < 0.02). Interannual variability in chl-*a* was only found in Bouzigues with 3 times more biomass in 2019 (p = 0.0007) than in 2017. Similar patterns were observed for chl-*b* and chl -*c* biomass, with twice as much chl-*b* in the samples collected 2019 samples than in the samples collected in 2017 (0.069 µg L^{-1} versus 0.026 µg L^{-1}; p=0.0001), and a more than two-fold increase in chl-*c* (0.103 ug L^{-1} versus 0.046 ug L^{-1}), particularly in Listel (p=0.039) and Bouzigues (p=0.0003).

Flow cytometry data showed an effect of the year factor on cells smaller than 3 µm (Fig.). Abundances of picoeukaryotes (<3 µm) (Supplementary Table 10), picocyanobacteria (<1 µm) (Supplementary Table 11 and 12) and bacteria (Supplementary Table 14) were higher in 2019 than in 2017. However, nanophytoplankton (3-20 µm) abundances decreased by 39% in 2019 (Supplementary Table 13). The abundance of total heterotrophic flagellates did not vary significantly among sites or between years, mean value 2 866 ± 291 cell mL^{-1}. Dinoflagellate and diatom abundances were affected by the year factor (df=1 and 35, pseudo-*F*=5.64, p=0.023), total values decreased by 60% in 2019 compared to 2017. These variations were linked to a 93% decrease in *Chaetoceros* abundance from 184 715 ± 66 846 to 12 483 ± 3 540 cells L^{-1} (Simper contribution: 77%, df=1 and 35, pseudo-F=8.73, p=0.0001) and a decrease that led to the disappearance of *Skeletonema* in Listel and Meze between 2017 and 2019. Diatom taxa were fewer in number at all sites sampled in 2019 with a maximum of 13 compared to 21 taxa identified in 2017. A marked increase in *Pseudo-nitzschia* (19 920 ± 10 513 to 50 562 ± 13 652 cells L^{-1}) with a Simper contribution of 8% and (df=1 and 35, pseudo-F=8.73, p=0.0001), *Leptocylindrus* (Simper contribution 7%), *Thalassionema*, and *Cylindrotheca* (1 837 ± 222 to

313 18 712 ± 12 010 cells L^{-1}) was observed in 2019 compared to 2017. This trend is especially
314 expressed in Bouzigues (Fig. 6). This result also reflects the higher diversity of dinoflagellate
315 taxa observed in 2019 (16 taxa) than in 2017 (12 taxa).
316 TFA contents in the $TPM_{0.7\text{-}20}$ samples were twice higher in 2019 (19.2 µg mg $TPM_{0.7\text{-}20}^{-1}$) than
317 in 2017 (9.9 µg mg $TPM_{0.7\text{-}20}^{-1}$; df=1 and 61, pseudo-*F*=17.1, p=0.0002) with no differences
318 among sites and year × site effects. The fatty acid composition of the $TPM_{0.7\text{-}20}$ samples differed
319 between years (df=3 and 76, pseudo-*F*=3.08, p=0.0001; Fig. S2) and, as determined by the
320 SIMPER analysis, explained 97% of the differences in the levels of 18:1n9, 18:0, 16:1, 18:2n6,
321 16:0, 14:0, 20:5n3 and 22:6n3. Twenty-six percent of the difference observed between years
322 was related to 18:1n9, a FA that was twice as abundant in 2017 (up to 24.1% of the TFA)
323 compared to 2019. The dissimilarity in the FA profiles observed between years was also
324 explained by higher values of 18:2n6 (representing up to 10.8% of TFA), and EPA (7%) in
325 2017. 18:2n6 and EPA were, respectively, 11.3% and 5% higher in 2017 than in 2019. The most
326 abundant FAs in the $TPM_{0.7\text{-}20}$ samples in 2019 were 16:1 and DHA which explained,
327 respectively, 13% and 4.3% of the dissimilarity shown by the SIMPER analysis.
328

329 **3.4 Territorial competition by worms**

330 The percent cover of tubeworms (*Ficopomatus enigmaticus*) on plates in 2019 showed a marked
331 increase in this species. Differences were observed among the sites (df=3 and 33, pseudo-
332 *F*=157, p=0.0001). Results showed similar cover of tubeworms (93.6 ± 1.5%) in Listel and
333 Bouzigues and a lower cover in Meze (83.2 ± 2.6%) ($p < 0.032$) and in Marseillan (23.6 ± 3.7%)
334 ($p < 0.0001$).
335

4. DISCUSSION

The aim of this study was to identify the environmental and trophic drivers of the decline in the recruitment of the Pacific oyster, *Crassostrea gigas*, in association with a heat wave. Our hypothesis that a heat wave has a negative effect on oyster recruitment by altering plankton diversity was confirmed. While oyster recruitment was normal in 2017, an unprecedented failure was observed in summer 2019 in the Mediterranean Thau lagoon. The atmospheric conditions during a heat wave have a strong direct effects on marine and lagoon environments that supply a variety of ecosystem services and valuable host species (Sarà et al. 2021). Temperature and salinity conditions are key ecological and physiological factors for *Crassostrea* larvae (His et al. 1989b, Baldwin & Newell 1995a, Devakie & Ali 2000, Troost et al. 2009). In controlled experimental settings, the entire larval life of *C. gigas*, including metamorphosis, showed a high tolerance to temperatures ranging from 17 °C to 32 °C at a salinity level of 34, with low mortality (≤10%) and the maximum growth rate at 32 °C(Rico-Villa et al. 2009). The physiological limits of temperature tolerance were therefore not reached in our experimental conditions and temperature was not the origin of the failure in this case. Salinity did not drop below 38 in either the 2017 or 2019 recruitment season, and intermittently reached more than 40 in 2019. *Crassostrea gigas* is an estuarine organism that tolerates a wide range of salinity (Nell & Holliday 1988), but no information is available in the literature on the upper salinity tolerance of the larval stage in real conditions. The high salinity in 2019 could represent the physiological salinity threshold for oyster larvae. Our results showed that the larval shell (prodissoconch) at the time of metamorphosis (PII) was smaller in 2019, suggesting a reduction in larval growth or faster achievement of metamorphosis competence in high salinity years. In agreement with Nell and Holliday (1988) who reported an optimal salinity range for larval

359 growth up to 27 and a very marked growth reductions at 31-39 (Nell & Holliday 1988), the
360 smaller observed PII size could be related to growth limitation under high salinity. Interestingly,
361 these authors reported no significant effect of salinity on larval survival between 19 and 39 but
362 the growth rate of larvae decreased markedly from 30 S (Helm & Millican 1977). Upper
363 tolerance limits of oysters to high salinity ranging from 35 S to 45 S should thus be further tested
364 in the laboratory including interactions with high temperature and different nutritional inputs
365 (His et al. 1989a).
366 The heat wave that occurred in 2019 resulted in large quantities of particulate matter and
367 chlorophyll biomass, but their quality appeared to be unfavorable for oyster recruitment. The
368 failure of oyster recruitment in 2019 could thus be linked to the change in the phytoplankton
369 community with low abundance of forage diatoms and high abundance of picoplanktonic
370 prokaryotes and eukaryotes, flagellates, and of the diatoms *Pseudo-Nitzschia* and
371 *Cylindrotheca*. However, the trophic environment was not characterized by a planktonic
372 community poor in fatty acids, and it was in fact richer than in 2017. Pediveliger larvae
373 accumulated the same quantity of fatty acids in 2019 as in 2017, but metamorphosis failures
374 were observed at all sites. We suggest that this failure may be linked to inappropriate trophic
375 conditions, which in turn, are mainly linked to the size of picoplankton species. These species
376 are poorly retained by the newly developed gills of young metamorphosed juveniles. Except for
377 larvae, the retention efficiency of bivalves for particles < 3-4 µm is low (Baldwin & Newell
378 1995b, Rosa et al. 2018). Our results suggest that the overabundance of small particles
379 (picoplanktonic prokaryotes and eukaryotes) could be critical for larval settlement and
380 metamorphosis. Higher chlorophyll biomass was observed in the nanophytoplankton fraction
381 during the heat wave of 2019 than in 2017, indicating changes in the phytoplankton community.

382 The heat wave was characterized by the increasing abundances of picocyanobacteria (Bec et al.
383 2005, Collos et al. 2009, Derolez et al. 2020b) and decreasing abundances of
384 nanophytoplankton. The Thau lagoon began an oligotrophication trajectory in the early 2000s
385 (Collos et al. 2009, Derolez et al. 2020a). This process caused a community shift due to a
386 reduction in nutrient loads since the 1970s thanks to improved wastewater treatment in the
387 watershed aimed at halting eutrophication (EC 1991a b, 2000). The reduction in nutrient loads
388 has been amplified by a decrease in total rainfall since the 2000s due to climate change (Derolez
389 et al. 2020a). Our results corroborate evidence that the proportion of small taxa, like
390 picoplankton, in the phytoplankton community, is increasing in coastal, marine and freshwater
391 ecosystems in response to global warming (Daufresne et al. 2009, Mousing et al. 2014, Pinckney
392 et al. 2015). Small phytoplankton cells have been observed to dominate in oligotrophic
393 environments (Irwin et al. 2006).
394
395 The high temperatures and high salinity in 2019 had a negative impact on trophic conditions for
396 larvae. However, recruitment failure appeared to be more linked to the ecological limitations of
397 the larvae at the time of their metamorphosis than to their physiological state. At the same time,
398 high temperatures and high salinity stimulated the development of the annelid *Ficopomatus*
399 *enigmaticus*, triggering a shift in community composition that is destructive for oyster
400 recruitment. We consequently hypothesize that these annelids are important territorial
401 competitors (Heiman & Micheli 2010, McQuaid & Griffiths 2014, Peria & Pernet 2019) and
402 trophic competitors of oyster larvae (Davies et al. 1989, Bruschetti et al. 2008, 2018, Pan &
403 Marcoval 2014) in shallow water and brackish habitats.

This study demonstrates, for the first time, an ecological process leading to the recruitment failure of the Pacific oysters due to an extreme heat wave. The oligotrophication trajectory of our study site combined with the effects of high water temperatures promoted variations in the phytoplankton communities that benefit picophytoplankton including cyanobacteria, that are likely unfavorable for the successful larval development of oysters until their juvenile metamorphosis (Lagarde et al. 2017). The present study thus reveals the ecological limits of the reproductive process of the Pacific oyster in the context of a heat wave in a Mediterranean lagoon. The heat wave phenomenon observed in 2019 severely disrupted the reproductive cycle of oysters in the Thau lagoon. In this context, the oyster nursery function within an oyster farming ecosystem can only be achieved or maintained when pico-, nano- and microphytoplankton communities are present and abundant and oysters can find favorable areas for larval development and optimize their recruitment. This study provides evidence that, in the conditions caused by a heat wave, the ecological limits of Pacific oyster larvae are narrower than their physiological limits. The effects of climate change, particularly the warming of waters in semi-enclosed basins, will certainly lead to problems in larval harvesting in the near futures. The information presented in this paper should help adapt oyster aquaculture, including husbandry practices, to a future marked by climate change.

5. Data and code availability

All data used in the current study and scripts used in our analysis are publicly available or were obtained by the corresponding author. This research benefited from the VELYGER Database: The Oyster Larvae Monitoring French Project (http://doi.org/10.17882/41888) and REPHY

Dataset - French Observation and Monitoring program for Phytoplankton and Hydrology in coastal waters. Metropolitan data. SEANOE (https://doi.org/10.17882/47248).

6. REFERENCES

Baldwin BS, Newell RI (1995a) Feeding rate responses of oyster larvae (*Crassostrea virginica*) to seston quantity and composition. J Exp Mar Bio Ecol 189:77–91.

Baldwin BS, Newell RI (1995b) Relative importance of different size food particles in the natural diet of oyster larvae (*Crassostrea virginica*). Mar Ecol Prog Ser 120:135–146.

Bassim S, Chapman RW, Tanguy A, Moraga D, Tremblay R (2015) Predicting growth and mortality of bivalve larvae using gene expression and supervised machine learning. Comp Biochem Physiol - Part D Genomics Proteomics 16:59–72.

Bec B, Collos Y, Souchu P, Vaquer A, Lautier J, Fiandrino A, Benau L, Orsoni V, Laugier T (2011) Distribution of picophytoplankton and nanophytoplankton along an anthropogenic eutrophication gradient in French Mediterranean coastal lagoons. Aquat Microb Ecol 63:29–45.

Bec B, Husseini-Ratrema J, Collos Y, Souchu P, Vaquer A (2005) Phytoplankton seasonal dynamics in a Mediterranean coastal lagoon: Emphasis on the picoeukaryote community. J Plankton Res 27:881–894.

Bouvy M, Got P, Domaizon I, Pagano M, Leboulanger C, Bouvier C, Carre C, Roques C, Dupuy C (2016) Plankton communities in the five Iles Eparses (Western Indian Ocean) considered to be pristine ecosystems. Acta oecologica- Int J Ecol 72:9–20.

Bower SM, Meyer SG (1990) Atlas of anatomy and histology of larvae and early juvenile stages of Japanese scallop *Patinopecten yessoensis*. Can Spec Publ Fish Aquat Sci 111:1–51.

448 Bruschetti CM, Addino M, Luppi T, Iribarne O (2018) Effects of nutrient enrichment and
449 grazing by an invasive filter feeder on phytoplankton biomass in a South West Atlantic
450 coastal lagoon. Biol Invasions 20:2245–2256.
451 Bruschetti M, Luppi T, Fanjul E, Rosenthal A, Iribarne O (2008) Grazing effect of the invasive
452 reef-forming polychaete *Ficopomatus enigmaticus* (Fauvel) on phytoplankton biomass in
453 a SW Atlantic coastal lagoon. J Exp Mar Bio Ecol 354:212–219.
454 Chapman PM (2012) Management of coastal lagoons under climate change. Estuar Coast Shelf
455 Sci 110:32–35.
456 Collos Y, Bec B, Jauzein C, Abadie E, Laugier T, Lautier J, Pastoureaud A, Souchu P, Vaquer
457 A (2009) Oligotrophication and emergence of picocyanobacteria and a toxic dino fl
458 agellate in Thau lagoon , southern France. J Sea Res 61:68–75.
459 Colombo SM, Wacker A, Parrish CC, Kainz MJ, Arts MT (2017) A fundamental dichotomy in
460 long-chain polyunsaturated fatty acid abundance between and within marine and terrestrial
461 ecosystems. Environ Rev 25:163–174.
462 Da Costa F, Robert R, Quéré C, Wikfors GH, Soudant P (2015) Essential Fatty Acid
463 Assimilation and Synthesis in Larvae of the Bivalve *Crassostrea gigas*. Lipids 50:503–
464 511.
465 Daufresne M, Lengfellner K, Sommer U (2009) Global warming benefits the small.
466 Davies BR, Stuart V, de Villiers M (1989) The filtration activity of a serpulid polychaete
467 population Ficopomatus enigmaticus (Fauvel) and its effects on water quality in a coastal
468 marina. Estuar Coast Shelf Sci 29:613–620.
469 Derolez V, Malet N, Fiandrino A, Lagarde F, Richard M, Ouisse V, Bec B, Aliaume C (2020a)
470 Fifty years of ecological changes: Regime shifts and drivers in a coastal Mediterranean

lagoon during oligotrophication. Sci Total Environ 732:139292.

Derolez V, Soudant S, Malet N, Chiantella C, Richard M, Abadie E, Aliaume C, Bec B (2020b) Two decades of oligotrophication: evidence for a phytoplankton community shift in the coastal lagoon of Thau (Mediterranean Sea, France). Estuar Coast Shelf Sci:106810.

Devakie MN, Ali AB (2000) Salinity-temperature and nutritional effects on the setting rate of larvae of the tropical oyster, *Crassostrea iredalei* (Faustino). Aquaculture 184:105–114.

EC (1991a) Council Directive 91/271/EEC Concerning Urban Waste-water Treatment.

EC (1991b) Council Directive 91/676/EEC of 12 December 1991 Concerning the Protection of Waters against Pollution Caused by Nitrates from Agricultural Sources.

EC (2000) Directive 200/60/EC of the European Parliament and of the Council of 23 October 2000 Establishing a Framework for Community Action in the Field of Water Policy.

Fiandrino A, Ouisse V, Dumas F, Lagarde F, Pete R, Malet N, Le Noc S, de Wit R (2017) Spatial patterns in coastal lagoons related to the hydrodynamics of seawater intrusion. Mar Pollut Bull 119:132–144.

Filgueira R, Guyondet T, Comeau LA, Tremblay R (2016) Bivalve aquaculture-environment interactions in the context of climate change. Glob Chang Biol 22:3901–3913.

Gagné R, Tremblay R, Pernet F, Miner P, Samain JF, Olivier F (2010) Lipid requirements of the scallop *Pecten maximus* (L.) during larval and post-larval development in relation to addition of *Rhodomonas salina* in diet. Aquaculture 309:212–221.

Glencross BD (2009) Exploring the nutritional demand for essential fatty acids by aquaculture species. 71–124.

Heiman KW, Micheli F (2010) Non-native Ecosystem Engineer Alters Estuarine Communities. Integr Comp Biol 50:226–236.

494 Helm MM, Millican PF (1977) Experiments in the hatchery rearing larvae. 11.
495 His E, Robert R, Dinet A (1989a) Combined effect of temperature and salinity on fed and
496 starved larvae of the Mediterranean mussel *Mytilus galloprovincialis* and the Japanese
497 oyster *Crassostrea gigas*. Mar Biol 100:455–463.
498 His E, Robert R, Dinet A (1989b) Marine Biology of the Mediterranean mussel *Mytilus*
499 *galloprovincialis* and the Japanese oyster *Crassostrea gigas*. Mar Biol 100:455–463.
500 Hixson SM, Arts MT (2016) Climate warming is predicted to reduce omega-3, long-chain,
501 polyunsaturated fatty acid production in phytoplankton. Glob Chang Biol 22:2744–2755.
502 Hobday AJ, Oliver ECJ, Gupta A Sen, Benthuysen JA, Burrows MT, Donat MG, Holbrook NJ,
503 Moore PJ, Thomsen MS, Wernberg T, Smale DA (2018) Categorizing and Naming Marine
504 Heatwaves. Oceanography 31:162–173.
505 Irwin AJ, Finkel ZOE V, Schofield OME, Falkowski PG (2006) Scaling-up from nutrient
506 physiology to the size-structure of phytoplankton communities. 28.
507 Jouzel J, Ouzeau G, Déqué M, Jouini M, Planton S, Vautard R (2014) Le climat de la France au
508 XXIe siècle (Volume 4), Scénarios régionalisés: édition 2014 pour la métropole et les
509 régions d'outre-mer.
510 Kermagoret C, Claudet J, Derolez V, Nugues MM, Ouisse V, Quillien N, Baulaz Y, Le Mao P,
511 Scemama P, Vaschalde D, Bailly D, Mongruel R (2019) How does eutrophication impact
512 bundles of ecosystem services in multiple coastal habitats using state-and-transition
513 models. Ocean Coast Manag 174:144–153.
514 Klauschies T, Bauer B, Aberle-Malzahn N, Sommer U, Gaedke U (2012) Climate change
515 effects on phytoplankton depend on cell size and food web structure. Mar Biol 159:2455–
516 2478.

Lagarde F, Fiandrino A, Ubertini M, Roque d'Orbcastel E, Mortreux S, Chiantella C, Bec B, Bonnet D, Roques C, Bernard I, Richard M, Guyondet T, Pouvreau S, Lett C (2019) Duality of trophic supply and hydrodynamic connectivity drives spatial patterns of Pacific oyster recruitment. Mar Ecol Prog Ser 632:81–100.

Lagarde F, Roque E, Ubertini M, Mortreux S, Bernard I, Fiandrino A, Chiantella C, Bec B, Roques C, Bonnet D, Miron G, Richard M, Pouvreau S, Lett C, Marbec IUMR (2017) Recruitment of the Pacific oyster *Crassostrea gigas* in a shellfish-exploited Mediterranean lagoon : discovery, driving factors and a favorable environmental window. Mar Ecol Prog Ser 578:1–17.

Lepage G, Roy CC (1984) Improved recovery of fatty acid through direct transesterification without prior extraction or purification. J Lipid Res 25:1391–1396.

Lloret J, Marín A, Marín-Guirao L (2008) Is coastal lagoon eutrophication likely to be aggravated by global climate change ? 78.

Lu Y, Yuan J, Lu X, Su C, Zhang Y, Wang C, Cao X, Li Q, Su J, Ittekkot V, Garbutt RA, Bush S, Fletcher S, Wagey T, Kachur A, Sweijd N (2018) Major threats of pollution and climate change to global coastal ecosystems and enhanced management for sustainability. Environ Pollut 239:670–680.

Marie D, Partensky F, Jacquet S, Vaulot D (1997) Enumeration and cell cycle analysis of natural populations of marine picoplankton by flow cytometry using the nucleic acid stain SYBR Green I. Appl Environ Microbiol 63:186–193.

Martel A, Hynes TMT, Buckland-Nicks J (1995) Prodissoconch morphology, planktonic shell growth, and site at metamorphosis in *Dreissena polymorpha*. Can J Zool 73:1835–1844.

McQuaid KA, Griffiths CL (2014) Alien reef-building polychaete drives long-term changes in

invertebrate biomass and diversity in a small, urban estuary. Estuar Coast Shelf Sci 138:101–106.

Météo-France (2019) 46,0 °C à Vérargues : nouveau record officiel de température observée en France. http://www.meteofrance.fr/actualites/74345599-c-est-officiel-on-a-atteint-les-46-c-en-france-en-juin

Mousing EA, Ellegaard M, Richardson K (2014) Global patterns in phytoplankton community size structure — evidence for a direct temperature effect. 497:25–38.

Nell JA, Holliday JE (1988) Effects of Salinity on the Growth and Survival of Sydney Rock Oyster (*Saccostrea commercialis*) and Pacific Oyster (Crassostrea gigas) Larvae and Spat. 68:39–44.

Neveux J, Lantoine F (1993) Spectrofluorometric assay of chlorophylls and phaeopigments using the least squares approximation technique. Deep Res Part I 40:1747–1765.

Pan J, Marcoval MA (2014) Top-Down Effects of an Exotic Serpulid Polychaete on Natural Plankton Assemblage of Estuarine and Brackish Systems in the SW Atlantic. J Coast Res 30:1226–1235.

Parrish CC (1999) Determination of Total Lipid, Lipid Classes, and Fatty Acids in Aquatic Samples. Lipids Freshw Ecosyst:4–20.

Peria J, Pernet B (2019) Tolerance to salinity and thermal stress by larvae and adults of the serpulid annelid Ficopomatus enigmaticus. Invertebr Biol 138:e12271.

Pinckney JL, Benitez-Nelson CR, Thunell RC, Muller-Karger F, Lorenzoni L, Troccoli L, Varela R (2015) Phytoplankton community structure and depth distribution changes in the Cariaco Basin between 1996 and 2010. Deep Sea Res Part I Oceanogr Res Pap 101:27–37.

Rico-Villa B, Pouvreau S, Robert R (2009) Influence of food density and temperature on

563 ingestion, growth and settlement of Pacific oyster larvae, *Crassostrea gigas*. Aquaculture
564 287:395–401.
565 Rosa M, Ward JE, Shumway SE (2018) Selective Capture and Ingestion of Particles by
566 Suspension-Feeding Bivalve Molluscs: A Review. J Shellfish Res 37:727–746.
567 Sarà G, Giommi C, Giacoletti A, Conti E, Mulder C, Mangano MC (2021) Multiple climate-
568 driven cascading ecosystem effects after the loss of a foundation species. Sci Total Environ
569 770:144749.
570 Scannell HA, Pershing AJ, Alexander MA, Thomas AC, Mills KE (2016) Frequency of marine
571 heatwaves in the North Atlantic and North Pacific since 1950. Geophys Res Lett 43:2069–
572 2076.
573 Schlegel RW, Oliver ECJ, Wernberg T, Smit AJ (2017) Nearshore and offshore co-occurrence
574 of marine heatwaves and cold-spells. Prog Oceanogr 151:189–205.
575 Sherr EB, Caron DA, Sherr BF (1993) Staining of heterotrophic protists for visualization via
576 epifluorescence microscopy. In: *Handbook of Methods in Aquatic Microbial Ecology*, 1st
577 Editio. Kemp PF, Sherr BF, Sherr EB, Cole JJ (eds) Lewis Publishers, p 213–227
578 Smaal AC, Ferreira JG, Grant J, Petersen JK, Strand Ø (2019) Goods and Services of Marine
579 Bivalves.
580 Sommer U, Adrian R, Bauer B, Winder M (2012) The response of temperate aquatic ecosystems
581 to global warming: novel insights from a multidisciplinary project. Mar Biol 159:2367–
582 2377.
583 Sonier R, Filgueira R, Guyondet T, Tremblay R, Olivier F, Meziane T, Starr M, LeBlanc AR,
584 Comeau LA (2016) Picophytoplankton contribution to Mytilus edulis growth in an
585 intensive culture environment. Mar Biol 163:1–15.

Thomas Y, Bacher C (2018) Assessing the sensitivity of bivalve populations to global warming using an individual-based modelling approach. Glob Chang Biol:1–18.

Thomas Y, Cassou C, Gernez P, Pouvreau S (2018) Oysters as sentinels of climate variability and climate change in coastal ecosystems. Environ Res Lett 13.

Trombetta T, Vidussi F, Mas S, Parin D, Simier M, Mostajir B (2019) Water temperature drives phytoplankton blooms in coastal waters. PLoS One 14:1–28.

Troost K, Gelderman E, Kamermans P, Smaal AC, Wolff WJ (2009) Effects of an increasing filter feeder stock on larval abundance in the Oosterschelde estuary (SW Netherlands). J Sea Res 61:153–164.

Villamagna AM, Angermeier PL, Bennett EM (2013) Capacity, pressure, demand, and flow: A conceptual framework for analyzing ecosystem service provision and delivery. Ecol Complex 15:114–121.

7. ACKNOWLEDGEMENTS

This research was supported by the Natural Sciences and Engineering Research Council of Canada (NSERC-Discovery Grant no.299100) to R.T and by the *Ressources Aquatiques Québec* Research Network (*Fonds de Recherche du Québec-Nature et Technologies*, #2014-RS-171172) and MITACS (FR37656) for the internships of ACM during her stay at IFREMER. This research was also fund by the VELYGER network. F.L. and R.T. thank the RECHAGLO international research group, co-funded by Ifremer and the Department of Fisheries and Oceans (DFO), and the *Institut France-Québec pour la coopération scientifique en appui au secteur Maritime* (IFQM) for encouragement, support, and exchanges with Canada. F.L., M.H. T.M.

and M.H. thank FREA, JSPS and Campus France/Ministry of Foreign Affairs for funding the scientific exchange needed for this study and the development of all the ideas presented by our group.

We thank Hélène Cochet, Serge Mortreux, Anaïs Crottier, Clarisse Hubert, Nabila Guenineche, Gabriel Devique, Hervé Violette, Elise Hatey, Camille Gianaroli and Nathalie Gauthier for logistic support in the field and technical contributions in the laboratory.

8. AUTHOR CONTRIBUTIONS

A.C.M. was involved in investigation, methodology, writing, data curation, formal analysis, and visualization. R.T. and F.L. were involved in conceptualization, funding acquisition, investigation, methodology, writing, data curation, formal analysis, visualization, and project administration. S.P. was involved in conceptualization, funding acquisition, investigation, methodology, writing and project administration. B.B was involved in conceptualization, funding acquisition, investigation, methodology, writing, data curation, formal analysis, and visualization. C.R. contributed to funding acquisition, methodology, writing, data curation and formal analysis. A.A and A.G. contributed to writing and interpretation. G.M. contributed to funding acquisition, investigation, methodology, writing and formal analysis. M.R., M.Ho, M.Ha. and T.M. contributed to conceptualization, investigation, methodology and writing.

9. COMPETING INTERESTS

The authors declare no competing interests.

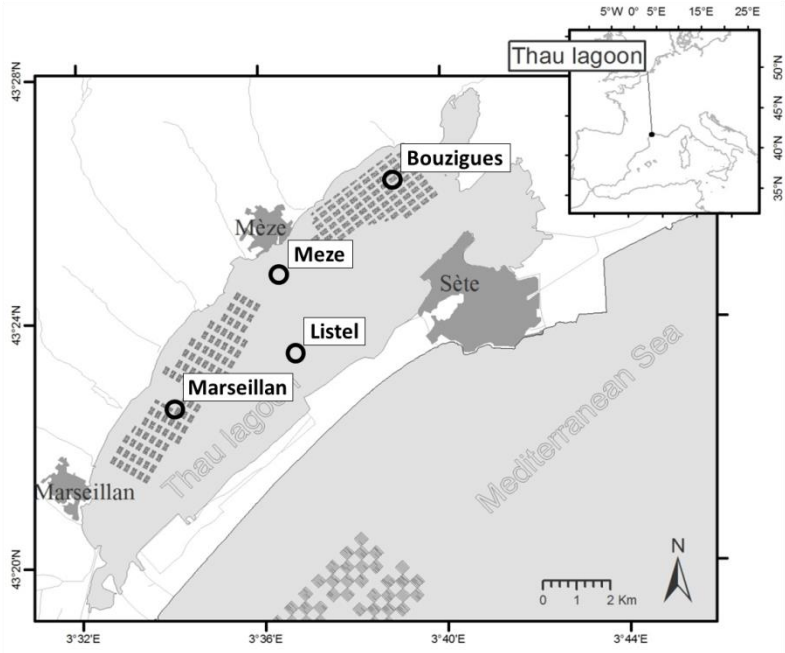

Fig. 1. The four sampling sites in the Thau lagoon. Marseillan and Bouzigues are located in the shellfish farming area; shaded areas indicate the location of shellfish culture areas. Meze and Listel are located outside the aquaculture area.

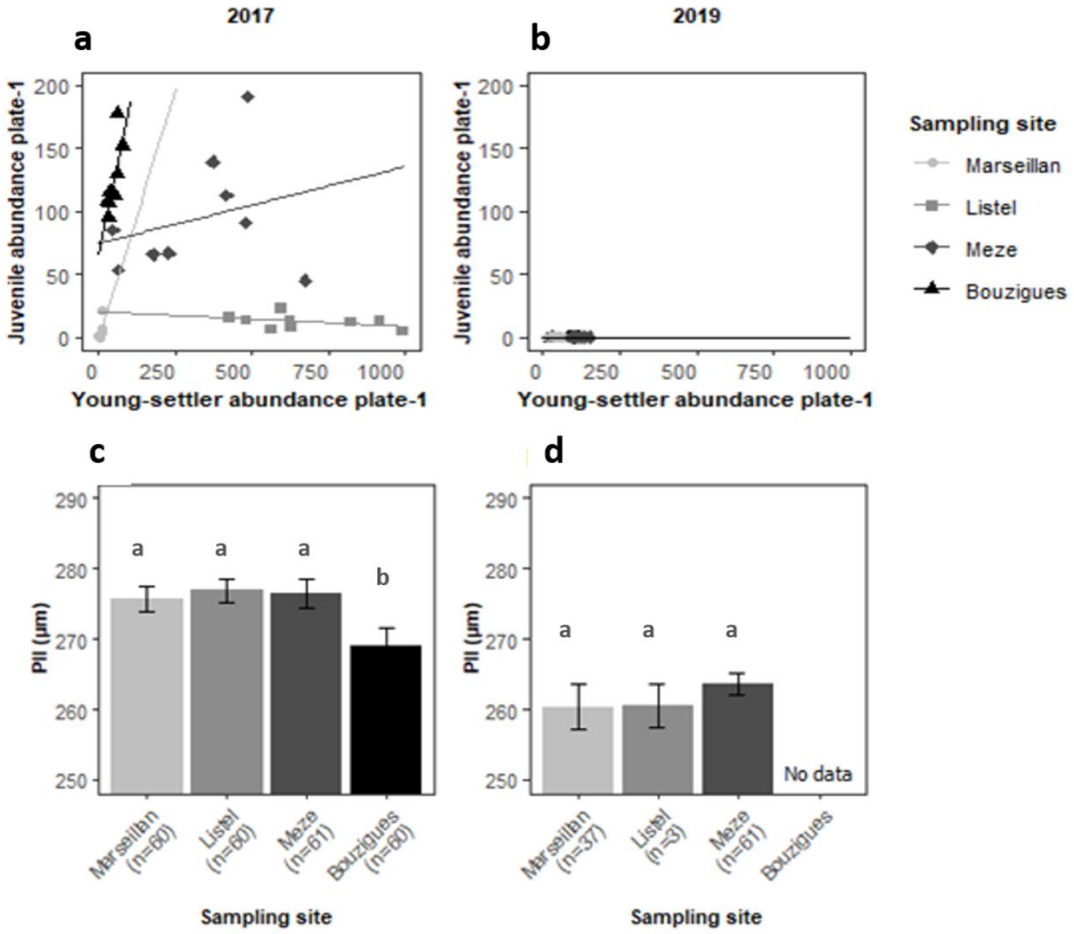

Fig. 2. Variability of oyster recruitment and prodissoconch II size according to the years 2017 (no heat wave) and 2019 (heat wave). *Crassostrea gigas* recruitment performance with young settlers (pediveligers + post-larvae) and juvenile abundance per collector plate observed at the four sampling sites during the summer recruitment events in (a) 2017 and in (b) 2019. Size at metamorphosis was estimated by the length of prodissoconch II shell (PII, µm ± SE) of juveniles sampled in (c) 2017 and (d) 2019. Different letters indicate significant differences between sites according to post-hoc multiple comparison tests after PERMANOVA.

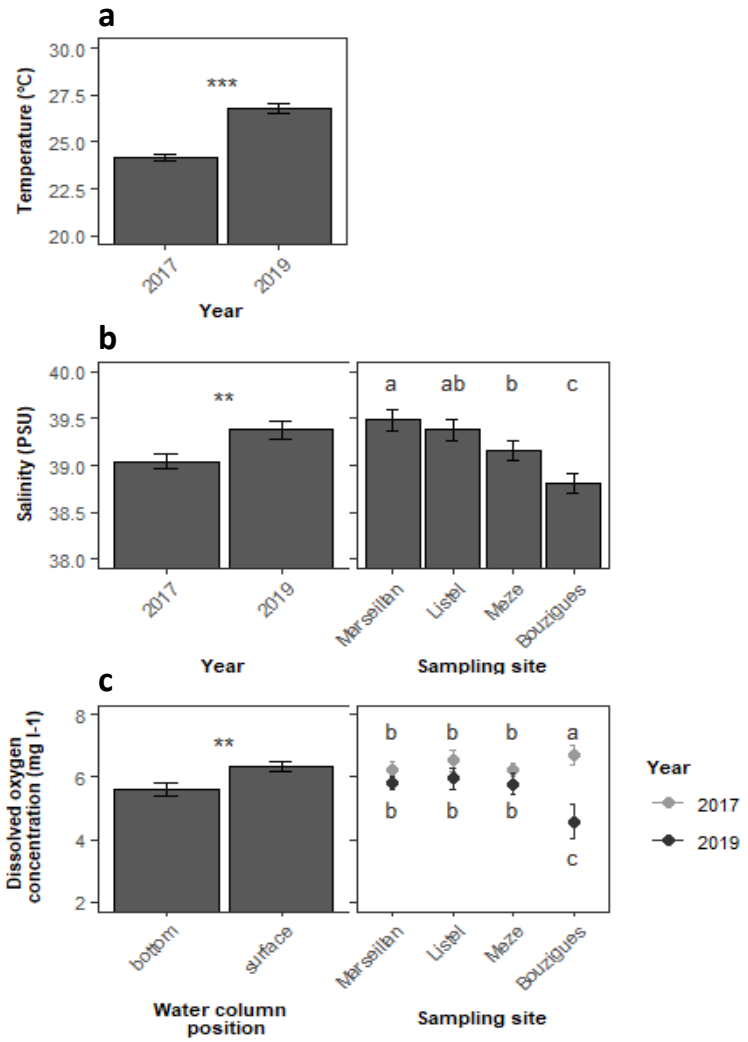

643

644 Fig. 3. Physico-chemical monitoring in 2017 (no heat wave) and 2019 (heat wave). (a) Mean
645 temperature (°C ± SE) per year (n = 40), (b) mean salinity (PSU ± SE) per year (n = 40) and per
646 sampling site (n = 20) and (c) mean dissolved oxygen concentration (mg L^{-1} ± SE) according to
647 the position of the sample in the water column (n = 40) and per year and sampling site (n = 10).
648 Stars indicate significant differences in parameter average per year (* $p \leq 0.05$, ** $p \leq 0.01$, ***
649 $p \leq 0.001$). Different letters indicate significant differences between sites according to post hoc
650 multiple comparison tests after PERMANOVA.

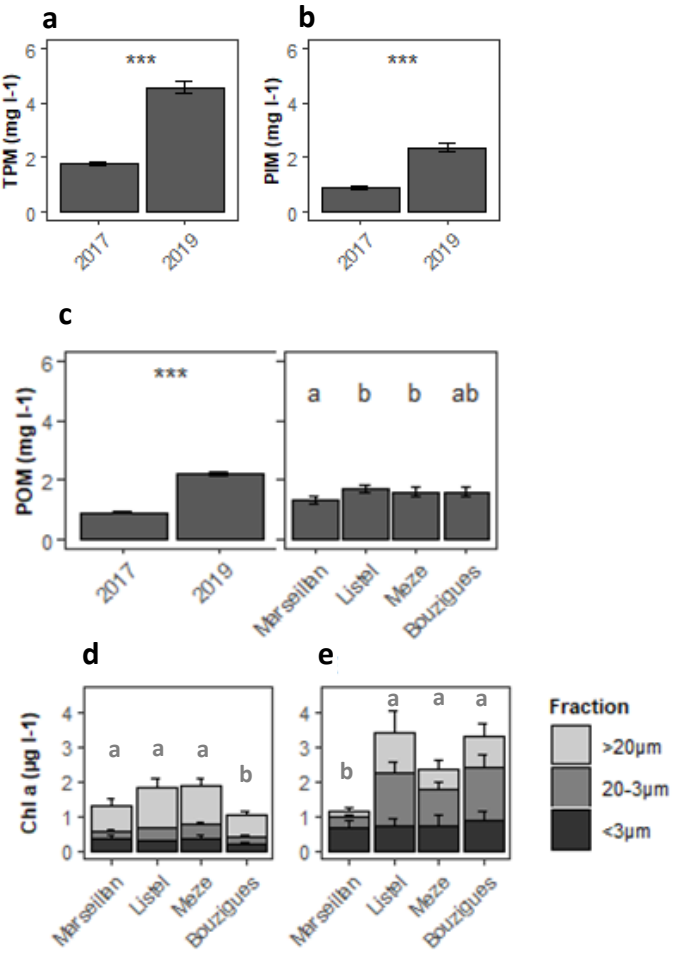

Fig. 4. Hydrobiological monitoring in 2017 (no heat wave) and 2019 (heat wave). Mean concentrations of (a) total particulate matter (TPM, mg L^{-1} ± SE), (b) particulate inorganic matter (PIM, mg L^{-1} ± SE) and (c) particulate organic matter (POM, mg L^{-1} ± SE) per year and sampling site (n = 5 per sampling site and year). Mean concentrations of chlorophyll-a (d, 2017 and e; 2019; µg L^{-1} ± SE), found in the picophytoplankton fraction (< 3 µm), the nanophytoplankton fraction (3 to 20 µm) and the microphytoplankton fraction (> 20 µm) per year and sampling site (n = 5 per sampling site, year and phytoplankton fraction). Stars indicate significant differences according to parameter average by year (* $p \leq 0.05$, ** $p \leq 0.01$, *** $p \leq 0.001$). Different letters indicate significant differences between sites according to post-hoc multiple comparison tests after PERMANOVA.

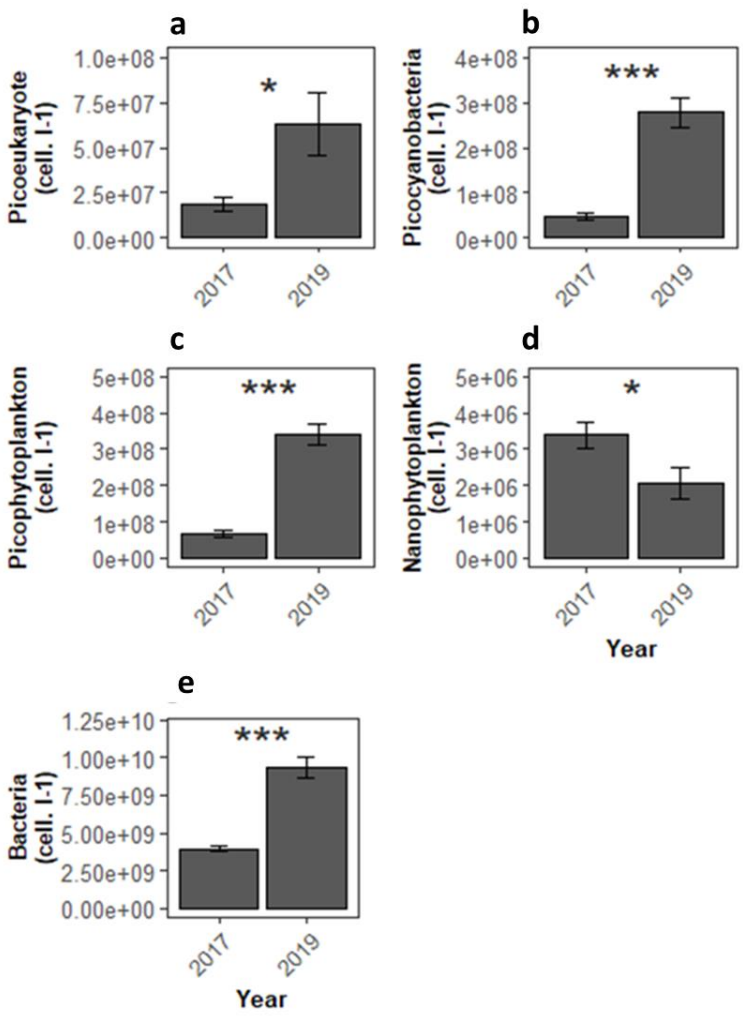

Fig. 5: Monitoring of picophytoplankton population in 2017 (no heat wave) and 2019 (heat wave). Average abundances for all sites of (a) photosynthetic picoeukaryotes, (b) picocyanobacteria, (c) picophytoplankton, (d) nanophytoplankton and (e) bacteria (cells L^{-1} ± SE) per year (n=20). Stars indicate significant differences according to parameter average by year (* $p \leq 0.05$, ** $p \leq 0.01$, *** $p \leq 0.001$).

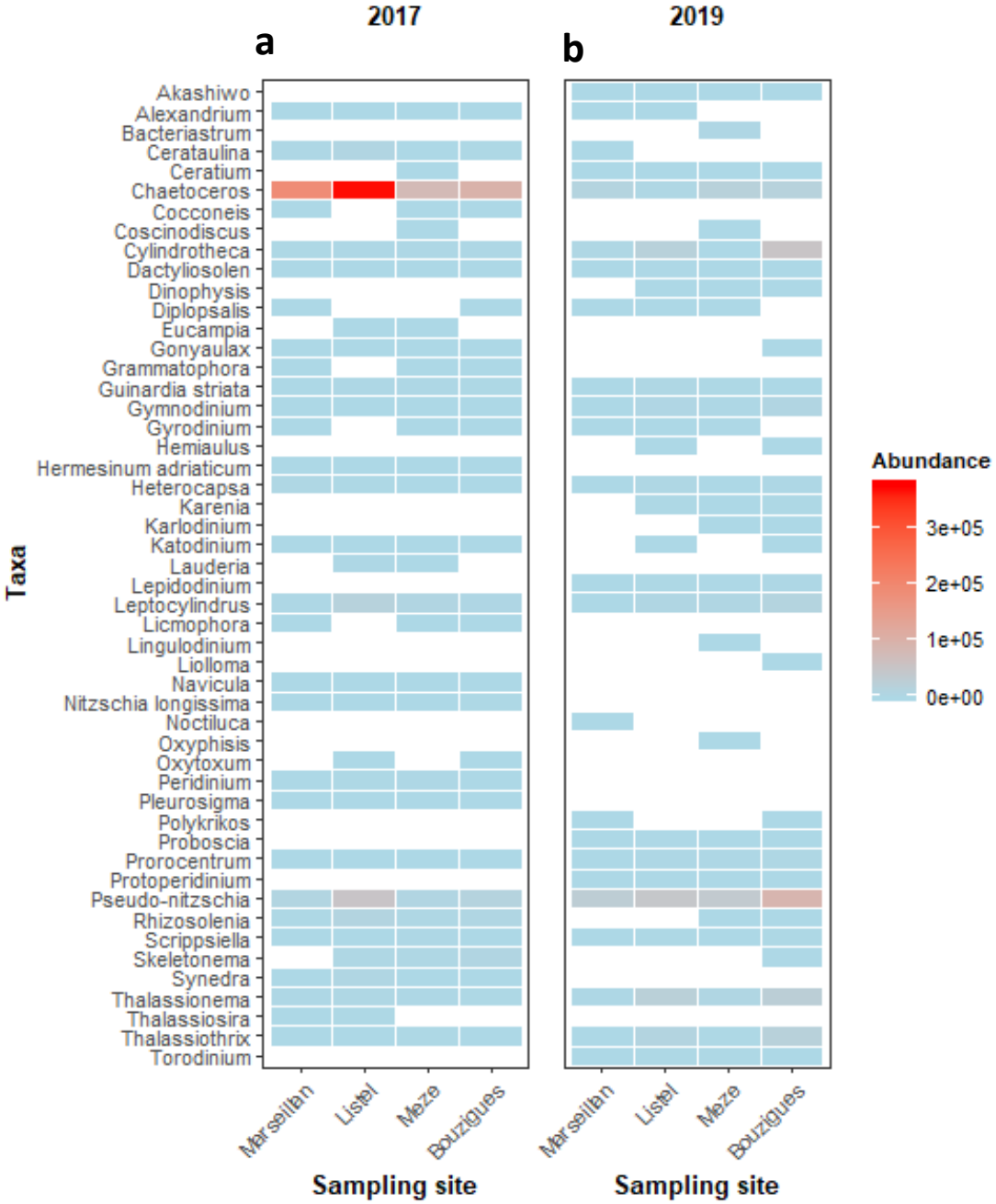

670

671 Fig. 6: Heatmap of microphytoplankton genera with changes in abundances in 2017 (no heat
672 wave) and 2019 (heat wave). Average phytoplankton abundance (cells L^{-1}) per taxon and
673 sampling site in (a) 2017 (n = 5) and (b) in 2019 (n = 4).

674

675 *Supplementary Table 1: Summary of the parameters analyzed characterizing the oyster larvae*

Variables	Description	Unit of measure	Abbreviation
Oyster variables			
Oyster pediveligers	*Abundance on collector plates*	*ind. plate-1*	*pediveligers*
Newly metamorphosed juveniles	*Abundance on collector plates*	*ind. plate-1*	*postlarvae*
Young settlers	*Abundance of pediveligers+ newly metamorphosed juveniles on collector plates*	*ind. plate-1*	*Young settlers*
Prodissoconch II size	*Measurement of prodissoconch maximum shell height along maximal dorsoventral axis of larvae or juvenile Pacific oysters*	*mm*	*PII size*
Total fatty acid in young settlers	*Total fatty acid contents in larvae (young settlers)*	*ng lavae-1*	*TFA*
Essential fatty acids	*Sum of essential fatty acids in larvae (docosahexaenoic acid (22:6ω3; DHA), eicosapentaenoic acid (20:5ω3; EPA) and arachidonic acid (AA))*	*ng lavae-1*	*EFA*

676

677 *Supplementary Table 2: Summary of the parameters analyzed characterizing the environment.*

Variables	Description	Unity	Abbreviation
Environmental variables			
Temperature	Discrete measure	°C	-
Salinity	Discrete measure	No unit	-
Oxygen concentration	Discrete measure	mg l^{-1}	-
Total particulate matter$_{0.7\text{-}20\mu m}$	Total particular pelagic material in the 0.7-20µm fraction	mg l^{-1}	$TPM_{0.7\text{-}20\mu m}$
Particulate organic matter$_{0.7\text{-}20\mu m}$	Particulate pelagic material in fraction the 0.7-20µm fraction	mg l^{-1}	$POM_{0.7\text{-}20\mu m}$
Particulate inorganic matter$_{0.7\text{-}20\mu m}$	Particulate inorganic pelagic material in the fraction 0.7-20µm fraction	mg l^{-1}	$PIM_{0.7\text{-}20\mu m}$
TFA content in $TPM_{0.7\text{-}20}$	TFA content in $TPM_{0.7\text{-}20}$	µg mg $TPM_{0.7\text{-}20}^{-1}$	
Total chlorophyll a	Total chlorophyll a biomass	µgChla l^{-1}	chloa
Total chlorophyll b	Total chlorophyll b biomass	µgChlb l^{-1}	chlob
Total chlorophyll c	Total chlorophyll c biomass	µgChlc l^{-1}	chloc
Picophytoplankton biomass	Chlorophyll a biomass in the <3µm fraction (picoeukaryotes)	µgChla l^{-1}	pico_chloa
Nanophytoplankton biomass	Chlorophyll a biomass in the 3-20µm fraction (nanoeukaryotes)	µgChla l^{-1}	nano_chloa
Picophytoplankton+ nanophytoplankton	Biomass	µgChla l^{-1}	nano_total_chloa
Microphytoplankton > 20µm	Biomass (microeukaryotes)	µgChla l^{-1}	micro_chloa
Bacteria	Abundance of picocyanobacteria (<1 µm)	10^6 cell. l^{-1}	bacteria
Total picoeukaryotes	Abundance	10^6 cell. l^{-1}	peuk_tot
picoeukaryotes+ cyanophycae	Abundance	10^6 cell. l^{-1}	pico_tot
Nanophytoplankton	Abundance	10^6 cell. l^{-1}	nano
cryptophyceae	Abundance	10^6 cell. l^{-1}	crypto
Nanophytoplankton + cryptophyceae	Abundance	10^6 cell. l^{-1}	nano_tot
Heterotrophic flagellates	Abundance	cell l^{-1}	HF
Ciliates	Abundance	cell l^{-1}	ciliates
Tintinnidae	Abundance	cell l^{-1}	tinti
Diatoms	Abundance	cell l^{-1}	diatom
Dinoflagellates	Abundance	cell l^{-1}	Dinoflagellate
Territorial competition by worms			
Worm coverage	Percent cover of tubeworms (Ficopomatus enigmaticus) on plates	%	-

678

679

Supplementary Table 3: multivariate PERMANOVA investigating site and year effect for Temperature

Source	df	SS	MS	Pseudo-F	P(perm)	Unique perms	P(MC)
site	3	7,087	2,3623	1,158	0,3305	9951	0,3335
year	1	135,72	135,72	66,53	0,0001	9825	0,0001
position	1	3,2	3,2	1,5686	0,2085	9805	0,217
sitexyear	3	0,3865	0,12883	0,063154	0,9764	9951	0,9754
sitexposition	3	2,573	0,85767	0,42042	0,7357	9950	0,7371
yearxposition	1	1,1045	1,1045	0,54142	0,4681	9828	0,473
sitexyearxposition	3	0,0865	0,028833	0,014134	0,9977	9955	0,9977
Res	64	130,56	2,04				
Total	79	280,72					

Supplementary Table 4: multivariate PERMANOVA investigating site, depth and year effect for salinity

Source	df	SS	MS	Pseudo-F	P(perm)	Unique perms	P(MC)
Site	3	5,331	1,777	7,5677	0,0002	9962	0,0004
Year	1	2,2445	2,2445	9,5587	0,0031	9805	0,0034
position	1	0,072	0,072	0,30663	0,5764	9733	0,5827
sitexyear	3	0,5245	0,17483	0,74457	0,5286	9960	0,5323
sitexposition	3	0,059	0,019667	0,083755	0,9666	9945	0,9679
yearxposition	1	0,1125	0,1125	0,47911	0,4824	9806	0,4966
sitexyearxposition	3	0,0805	0,026833	0,11428	0,9545	9942	0,9503
Res	64	15,028	0,23481				
Total	79	23,452					

Supplementary Table 5: multivariate PERMANOVA investigating site, depth and year effect for oxygen

Source	df	SS	MS	Pseudo-F	P(perm)	Unique perms	P(MC)
site	3	3,8333	1,2778	1,3099	0,2739	9944	0,27
year	1	15,878	15,878	16,277	0,0004	9825	0,0001
position	1	10,039	10,039	10,292	0,002	9854	0,0018
sitexyear	3	10,01	3,3366	3,4205	0,0215	9947	0,0217
sitexposition	3	3,8499	1,2833	1,3156	0,2758	9955	0,2805
yearxposition	1	3,3048	3,3048	3,388	0,0708	9812	0,0682
sitexyearxposition	3	1,7959	0,59865	0,6137	0,6012	9955	0,5985
Res	64	62,43	0,97547				
Total	79	111,14					

Supplementary Table 6: multivariate PERMANOVA investigating site and year effect for TPM

Source	df	SS	MS	Pseudo-F	P(perm)	Unique perms	P(MC)
site	3	1,493	0,49767	0,28089	0,8424	9962	0,8364
year	1	207,48	207,48	117,1	0,0001	9839	0,0001
sitexyear	3	2,0244	0,67479	0,38085	0,7691	9958	0,7708
Res	100	177,18	1,7718				
Total	107	388,6					

Supplementary Table 7: multivariate PERMANOVA investigating site and year effect for PIM

Source	df	SS	MS	Pseudo-F	P(perm)	Unique perms	P(MC)
site	3	0,11747	0,039156	0,039431	0,9901	9949	0,9904
year	1	54,939	54,939	55,325	0,0001	9814	0,0001
sitexyear	3	0,33001	0,11	0,11077	0,957	9958	0,9508
Res	100	99,303	0,99303				
Total	107	154,73					

Supplementary Table 8: multivariate PERMANOVA investigating site and year effect for POM

Source	df	SS	MS	Pseudo-F	P(perm)	Unique perms	P(MC)
site	3	1,4638	0,48793	2,796	0,0429	9952	0,0407
year	1	48,888	48,888	280,15	0,0001	9824	0,0001
sitexyear	3	1,193	0,39765	2,2787	0,0834	9952	0,0832
Res	100	17,451	0,17451				
Total	107	69,327					

Supplementary Table 9: multivariate PERMANOVA investigating site, size and year effect for CHLOA

Source	df	SS	MS	Pseudo-F	P(perm)	Unique perms	P(MC)
site	3	3,35	1,1167	3,9887	0,0088	9958	0,0088
year	1	3,6519	3,6519	13,045	0,0003	9848	0,0007
taille	2	1,8257	0,91286	3,2608	0,0401	9953	0,0456
sitexyear	3	2,9083	0,96945	3,4629	0,0167	9953	0,0175
sitexsize	6	1,984	0,33066	1,1811	0,3199	9933	0,3246
yearxsize	2	5,0665	2,5333	9,0488	0,0004	9951	0,0004
sitexyearxsize	6	0,84964	0,14161	0,50582	0,8156	9949	0,8092
Res	96	26,876	0,27995				
Total	119	46,512					

Supplementary Table 10: multivariate PERMANOVA investigating site and year effect for PEUK_TOT

Source	df	SS	MS	Pseudo-F	P(perm)	Unique perms	P(MC)
site	3	1,2885E+16	4,2951E+15	1,3441	0,2784	9945	0,2768
year	1	1,959E+16	1,959E+16	6,1306	0,0155	9835	0,0187
sitexyear	3	2,6684E+15	8,8948E+14	0,27835	0,8512	9952	0,8401
Res	32	1,0226E+17	3,1955E+15				
Total	39	1,374E+17					

Supplementary Table 11: multivariate PERMANOVA investigating site, size and year effect for CYAN

Source	df	SS	MS	Pseudo-F	P(perm)	Unique perms	P(MC)
site	3	2,552E+16	8,5068E+15	0,7044	0,5664	9949	0,5635
year	1	5,3384E+17	5,3384E+17	44,205	0,0001	9851	0,0001
sitexyear	3	1,2146E+16	4,0486E+15	0,33524	0,8082	9953	0,797
Res	32	3,8645E+17	1,2077E+16				
Total	39	9,5796E+17					

Supplementary Table 12: multivariate PERMANOVA investigating site, size and year effect for PICO

Source	df	SS	MS	Pseudo-F	P(perm)	Unique perms	P(MC)
site	3	2,3685E+15	7,8951E+14	0,083154	0,9729	9939	0,9697
year	1	7,5797E+17	7,5797E+17	79,832	0,0001	9841	0,0001
sitexyear	3	3,7254E+15	1,2418E+15	0,13079	0,9431	9944	0,938
Res	32	3,0383E+17	9,4946E+15				
Total	39	1,0679E+18					

Supplementary Table 13 : multivariate PERMANOVA investigating site, size and year effect for NANO

Source	df	SS	MS	Pseudo-F	P(perm)	Unique perms	P(MC)
site	3	1,2396E+12	4,1319E+11	0,13497	0,9421	9944	0,9377
year	1	1,7765E+13	1,7765E+13	5,8032	0,0196	9837	0,0175
sitexyear	3	2,0028E+13	6,6759E+12	2,1807	0,1051	9950	0,1082
Res	32	9,7961E+13	3,0613E+12				
Total	39	1,3699E+14					

Supplementary Table 14 : multivariate PERMANOVA investigating site, size and year effect for BACT_TOT

Source	df	SS	MS	Pseudo-F	P(perm)	Unique perms	P(MC)
site	3	1,622E+19	5,4066E+18	0,93657	0,4508	9949	0,4387
year	1	2,909E+20	2,909E+20	50,392	0,0001	9839	0,0001
sitexyear	3	1,0607E+19	3,5358E+18	0,61249	0,6213	9957	0,6151
Res	32	1,8473E+20	5,7728E+18				
Total	39	5,0246E+20					

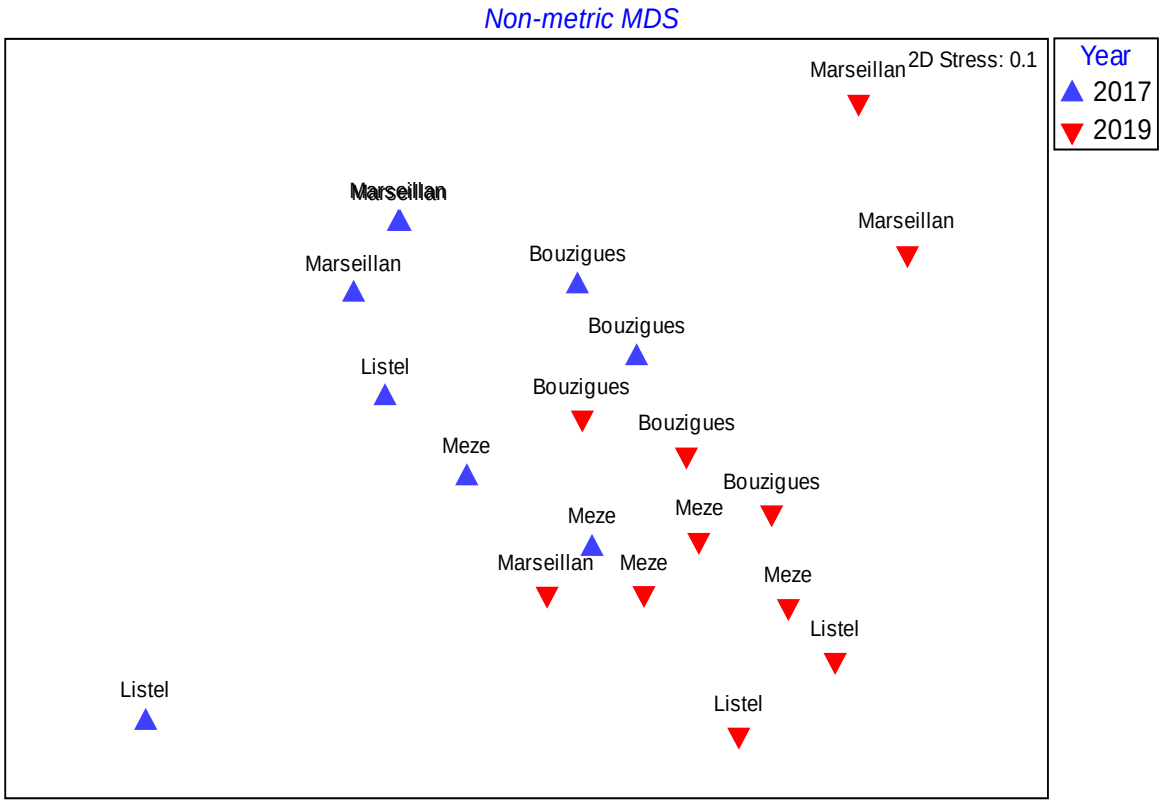

805

806 *Supplementary Figure 1. Non-metric multi-dimensional scaling of the Euclidean similarity matrix based on the relative*
807 *abundance of fatty acid profiles measured in young settlers larvae collected in 2017 and 2019 at each sampling sites in the*
808 *Thau lagoon.*

809